IEEE Access
Multidisciplinary | Rapid Review | Open Access Journal

Received February 11, 2020, accepted February 27, 2020, date of publication March 11, 2020, date of current version March 27, 2020.

Digital Object Identifier 10.1109/ACCESS.2020.2980043

Routing Void Prediction and Repairing in AUV-Assisted Underwater Acoustic Sensor Networks

ZHIGANG JIN[1], QINYI ZHAO[1], AND YONGMEI LUO[2]
[1]School of Electrical and Information Engineering, Tianjin University, Tianjin 300072, China
[2]School of Computer Science and Technology, Tianjin University, Tianjin 300072, China

Corresponding author: Yongmei Luo (luoyongmei@tju.edu.cn)

This work was supported by the National Natural Science Foundation of China (NSFC) under Project 61571318, Project 61862020, Project 61861014, and Project 61701335.

ABSTRACT Underwater Acoustic Sensor Networks have attracted much attention due to various applications. However, routing voids lead performance degradation of UASNs in terms of network connectivity and packet delivery ratio. In this paper, we propose a Routing Void Prediction and Repairing (RVPR) algorithm in AUV-assisted UASNs, which utilizes AUVs to carry sensor nodes to repair the routing voids when foreseeing the occurrence of voids. First, the repair position is calculated based on Particle Swarm Optimization algorithm by maximizing the connectivity of the void area and minimizing the AUV moving distance. Then, the routing void prediction based on Markov chain model is proposed to ensure that the AUVs come to the repair task before the voids have already formed. Next, we design a task selecting rule to let the AUVs choose the most important and urgent repair task. Lastly, RVPR applies an energy-efficient interaction mechanism among nodes and AUVs, which guarantees reliable operation of the algorithm. In the simulation, the RVPR algorithm is applied in several different types of routing protocols (HHVBF, QELAR, EAVARP). The simulation results show that RVPR algorithm improves the protocol performances in terms of the packet delivery ratio and the link connection. More specifically, when there are 100 nodes deployed in the network, the packet delivery ratio of HHVBF, EAVAPR and QELAR employing RVPR are increased by 29.4%,79% and 65% respectively.

INDEX TERMS Underwater acoustic sensor networks, routing voids, autonomous underwater vehicle.

I. INTRODUCTION

Three quarters of the Earth's surface is covered by oceans, which contain 97 per cent of the Earth's water. Moreover, the market value of marine and coastal resources and industries is estimated at $3 trillion per year or about 5 per cent of global GDP [1]. Thus, Underwater Acoustic Sensor Networks (UASNs) are becoming a promising technology for its wide applications on ocean monitoring, underwater exploration and oceanography data gathering [2]–[4].

However, it is challenging to build UASNs. One of the main reasons is that there is serious attenuation of electromagnetic waves underwater, which makes acoustic communication become the most effective method for long-distance communication [5]. Thus, it is important to consider the characteristics of underwater acoustic communication when designing algorithms and protocols for UASNs. Another reason is the limited energy of nodes. In UASNs, nodes deployed underwater are difficult to be charged or replaced batteries [6]. When individual nodes are exhausted due to uneven energy consumption, there will be routing voids in the network.

Obviously, the routing voids reduce network connectivity significantly, and therefore, the nodes around the routing void cannot find a relay node, which results in the reduction of packet delivery ratio and even the paralysis of the network. In UASNs, since nodes are usually sparsely deployed, the damage caused by routing voids is more obvious than that in the traditional wireless sensor networks.

There have emerged many works to solve routing voids problem underwater. Void-aware routing protocols are proposed to find a path to the sink bypassing the void area [7].

The associate editor coordinating the review of this manuscript and approving it for publication was Chakchai So-In.

Topology control algorithms based on the depth adjustment ability of the nodes are introduced to recover the connectivity in the communication void region [8]. There are also techniques taking a benefit of redundant overlapping and repairing a coverage hole during network operation [9].

However, the existing methods just solve the immediate void problem. When the routing voids are formed, in the existing studies, the nodes around the voids will start to be rather busy and quickly run out of energy. Therefore, the routing voids will expand quickly once they have already formed. As a result, the network will paralyze soon. Thus, the new direction of introducing new nodes in the network should be considered.

Autonomous Underwater Vehicles (AUVs) are rechargeable and can operate autonomously, which make them well suited to assist UASNs performing tasks, such as data collection, marine environment monitoring and localization. Reference [10] proposes a new underwater routing scheme named AUV-aided underwater routing protocol (AURP). It uses multiple AUVs as relay nodes from gateway nodes to sinks, which achieves a high delivery ratio and low energy consumption.

In recent years, there have been more and more researches on AUV autonomous operation [11], [12]. Reference [13] introduces a new method of load separation from the head of AUV. A set of transform models for the beginning position of the separated load and the carrier are deduced based on the dynamic equations. Reference [14] carries out numerical study on the store separation from the weapon bay of a BWB underwater glider, which is supported by the computational fluid mechanics and the six-degree-of-freedom model. Motived by AUV's load separation technology, we introduce AUVs to carry and deploy nodes to repair the routing voids.

In this paper, we propose a Routing Void Prediction and Repairing (RVPR) algorithm in AUV-assisted UASNs. The RVPR algorithm enables nodes to predict routing voids nearby, and then they ask AUVs to come in advance repairing the voids in time. Therefore, the algorithm does not require redundant or mobility of sensor nodes. Also, RVPR can still improve the performance of routing protocols even if they do not consider routing voids. The main contributions of this paper can be summarized as follows:

(1) RVPR algorithm takes full advantage of AUV's high energy, strong mobility and ability to carry objects and separate from the loads. In addition to daily work, the AUV can dynamically repair routing voids in UASNs to increase the network performance.
(2) To calculate the position of void repairing, RVPR establishes the objective functions by maximizing the connectivity of the void area and minimizing the AUV moving distance. Moreover, the sound propagation characteristics underwater are taken into account. The position of the AUV deploying nodes is calculated based on Particle Swarm Optimization (PSO) algorithm.
(3) Since the speed of the AUV is slow, in order to ensure that the AUV repairs the voids in time, it needs to come to the repair position before the voids have already formed. Thus, a routing void prediction model is proposed based on Markov chain.
(4) To guarantee the effect of RVPR, we propose a reliable and energy-saving information interaction mechanism among nodes and AUVs.
(5) The proposed RVPR algorithm is distributed, which can be easily employed with any routing protocols.

The rest of this paper is organized as follows: in Section II, the existing void repairing algorithms and protocols for UASNs are studied. In Section III and IV, the RVPR algorithm is described in detail. The simulation results are shown and discussed in Section V. Finally, we conclude this paper in Section VI.

II. RELATED WORK

In this section, we first review the shortcomings of traditional routing protocols in handling routing voids. Then we introduce the existing protocols and algorithms dealing with routing voids. Meanwhile, we summarize their advantages and disadvantages and existing problems.

VBF [15], HHVBF [16] and DBR [17] are traditional routing protocols in UASNs based on greedy algorithm. They all have multiple relay nodes, which consume a lot of energy. Furthermore, the idea of the greedy algorithm makes the nodes consume energy unevenly. In other words, nodes that continue to be the forwarders will exhaust energy prematurely. Thus, routing voids cannot be solved or avoided when applying traditional routing protocols.

To deal with the routing voids, a lot of studies have been done. Some routing protocols attempt to delay the generation of voids or bypass routing voids. QELAR proposed in [18] is a machine-learning-based routing protocol for energy-efficient and lifetime-extended underwater sensor network. In contrast to routing protocols based on the greedy algorithm, QELAR can select the next hop according to the residual energy of neighbors. Thus, the energy consumption is more even and the generation of routing voids can be delayed when applying QELAR. In [19], an energy-aware and void-avoidable routing protocol (EAVARP) is proposed. EAVARP first builds concentric shells around the sink node and distributes different layers to sensor nodes. Then, packets can be forwarded based on different concentric shells through opportunistic directional forwarding strategy (ODFS) even if there are voids. Although EAVARP avoids routing voids, the main idea is to find a path bypassing the void area, which increases the transmission delay and expands the voids over time.

Others try to solve the void problem equipping with the depth adjustment mechanism. Reference [20] proposes the centralized topology control (CTC) and the distributed topology control (DTC) mechanisms for long-term non-time-critical underwater sensor networks, which can organize the network via depth adjustment of some nodes. The topology control mechanisms can reduce the impact of communication void region in the network performance. In [21], the depth

adjustment is also used to improve the network connectivity and forward data where the greedy geographic routing fails. However, node movement consumes lots of additional energy which is already limited in UASNs. Moreover, the algorithms only consider the voids caused by dynamic topology changes, and do not take into account the voids because of the early exhaustion of nodes.

There are also techniques taking a benefit of redundant overlapping. On energy hole and coverage hole avoidance technique in underwater wireless sensor networks is proposed in [9]. It can repair coverage holes as well as energy holes during network operation by moving nodes from redundant coverage areas to the hole areas. However, the nodes in UASNs are usually sparse due to the long communication distance and the high cost of the nodes. Thus, node redundancy deployment is rarely achieved underwater.

In conclusion, the above ideas have some deficiencies. The void-aware routing protocols are proposed to bypass the void area, which increase the transmission delay and expand the voids over time. Although many algorithms that maximize coverage and connectivity can delay the occurrence of routing voids to some extent, it takes a lot of additional energy using the mobility of special nodes. Also, the algorithms deploying a lot of redundant nodes are costly to repair the routing voids. Therefore, it is necessary to find new solutions for routing voids underwater.

Recently, there have emerged a few works on handling the routing voids with the assistance of the AUV as its technology matures and improves [22]. In [23], a mobicast routing protocol for Underwater Sensor Networks is proposed. In the routing protocol, all possible sensor nodes near the AUV form a 3-D geographic zone is called a 3-D zone of reference (3-D ZOR). The main problem the routing protocol solved is how to efficiently collect data from sensor nodes within a 3-D ZOR while those sensor nodes are usually sleep for a long period. To consider the characteristics of UASNs and solve the void problem, an ''apple slice'' technique is used in the 3-D ZOR to build multiple segments to surround the void. When the delivery is obstructed by voids, the segment expands to a larger size and allows the packets to be sent to the AUV along the path bypassing the void area. However, similar to the void-avoided routing protocols, the expanded segment will involve more nodes that participate in routing, which leads to void expansion eventually.

To address the issues above, we propose the RVPR algorithm in this paper, which aims at repairing the routing voids when foreseeing void occurrence in AUV-assisted UASNs. Also, in RVPR, the voids can be repaired before it is already formed to avoid the expansion of the void area.

III. PRELIMINARIES

In this section, we firstly state the problem that RVPR solves, which also includes the system model. Then, the acoustic communication model is introduced and the routing void index is defined. These concepts and definitions are the basis for the details of RVPR in the next chapter. Finally, we present the basic idea of RVPR.

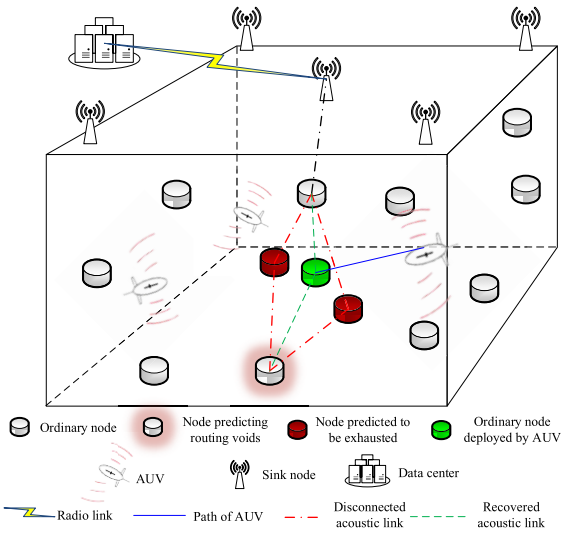

FIGURE 1. Network scenario.

A. PROBLEM STATEMENT

The network scenario is shown as Fig.1, which mainly consists of three members:

- Ordinary node - a node that can generate, receive and send packets. In RVPR, ordinary nodes calculate the positions repairing routing voids and predict the voids. When routing voids are predicted to occur, ordinary nodes send a task request to the AUV.
- Sink node - a node that collects packets from ordinary nodes and sends the packets to the data center.
- AUV - a vehicle that works underwater. It is rechargeable and can move flexibly. In RVPR, the AUV dynamically selects tasks, carrying and deploying ordinary nodes to the specified positions to repair routing voids.

In RVPR, ordinary nodes and AUVs are evenly distributed in the 3D water space. Ordinary nodes transmit packets upward to sink nodes located on the water surface. Each AUV carries an ordinary node and performs its own daily task (such as data collection, marine environment monitoring and localization.). When individual nodes are exhausted, there will be routing voids resulting in difficulty to find forwarders to the sink. The goal of RVPR is to predict the occurrence of routing voids and schedule the nearest AUV to the designated position in advance in order to repair the voids in time.

For routing void prediction and repairing, the overall task involves four subtasks. The first is to establish the objective functions by maximizing the connectivity of the void area and minimizing the AUV moving distance. The positions of the AUV deploying nodes are calculated based on the PSO algorithm. The second is to predict the routing voids based on Markov chain model. The third is to devise the task selecting

rule taking into account routing voids, node importance and AUV moving distance. The last is to design the energy-saving information exchange mechanism among ordinary nodes and AUVs.

The realization of our algorithm is based on the following assumptions:

(1) The sink nodes can obtain their own location information via GPS. The ordinary nodes obtain their own location information through the existing location service such as [24] and [25]. And the AUVs can get their location information by positioning device and GPS [26].
(2) Ordinary nodes can update the information of their neighbors by overhearing the underwater acoustic channel.
(3) The speed of AUVs is known.

B. ACOUSTIC COMMUNICATION MODEL

The path loss in the underwater acoustic channel can be estimated by Thorp model as follows [27]:

$$TL[dB] = \chi \log(1000 \times r) + \alpha(f) \cdot r \tag{1}$$

where χ is a parameter used to calculate the extended loss. Commonly used values are $\chi = 10$ for cylindrical spreading and $\chi = 20$ for spherical spreading. r is the distance between the sender node and the receiver node. $\alpha(f)$ is the absorption coefficient, which is related to the communication frequency:

$$\alpha(f)[dB/km] = \frac{0.11 \times f^2}{1+f^2} + \frac{44.0 \times f^2}{4100+f^2} + 2.75 \times 10^{-4} f^2 + 0.003 \tag{2}$$

In order to ensure the link quality, we compute the signal-to-noise ratio in acoustic channel as follows, which should be larger than the detection threshold of the receiver [28]:

$$SNR = SL - TL - NL + DG \geq Th_{receiver} \tag{3}$$

where SL is the signal level of the source node, TL is the transmission loss and DG is the directional gain. NL is the noise level, which includes underwater turbulence, shipping activity, wave and thermal noise. For practical applications, NL can be approximated as [29]:

$$NL = \eta_0 - \eta \cdot \log(f) \tag{4}$$

where the constant level η_0 is taken to be 50 dB re μ Pa and η is 18 dB/decade.

C. ROUTING VOID INDEX

Energy consumption of nodes is unbalanced when traffic load is uneven. Thus, busy nodes usually exhaust their energy early. The premature death of several nodes makes it difficult for their neighbors to find a relay node, which is called routing void phenomenon.

The routing void model is shown as Fig.2. We can see that the occurrence of routing voids means that within node communication range, all the neighbor nodes located in a certain direction or directions shut down. For example, n_4, n_5 and n_7 located in the upper right of n_2 exhaust their energy, which make n_2 unable to forward packets to the sink. In Fig.3, we approximate the node communication model as a sphere for the convenience of analysis, which is equally divided into eight areas I-VIII. Based on the above analysis, we can conclude that if all neighbors in any area run out of energy, it means that routing voids occur very likely. Thus, we define the routing void index based on this characteristic to describe the severity of voids.

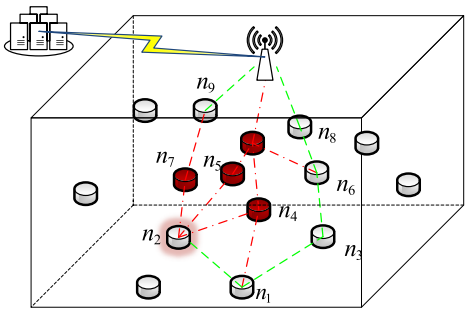

FIGURE 2. Routing void model.

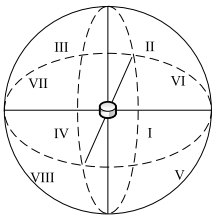

FIGURE 3. Node communication model. The approximated sphere is divided into eight parts centered on the nodes. The top four are counted as I-IV in a counterclockwise order, and the bottom four are counted as V-VIII in a counterclockwise order.

If the energy of all neighbor nodes in the same area is below the threshold, the area becomes a low-energy warning area. The more adjacent warning areas (adjacent areas refer to the areas share common faces), the more serious the routing voids. Thus, the routing void index is defined as follows:

$$\alpha = \frac{x}{n} \tag{5}$$

where x is the number of adjacent low-energy warning areas with the largest total volume, and n is the total number of areas. We can see from (5) that if the value of α becomes larger, the routing voids is severer.

For example, the routing void index of node in Fig.4(a) and Fig.4(b) is 1/8. This is because in Fig.4(a), there is only one low-energy warning area. Although there are two warning areas in Fig.4(b), area IV and VI are not adjacent. Similarly, the routing void index of node in Fig.4(c) and Fig.4(d) is 2/8. The reason is that there are two adjacent warning areas III and IV, of which the total volume is the largest.

Considering that the deployment of nodes is sparse underwater, the 8 areas may not all contain nodes even when the network connectivity is in good condition. In the following

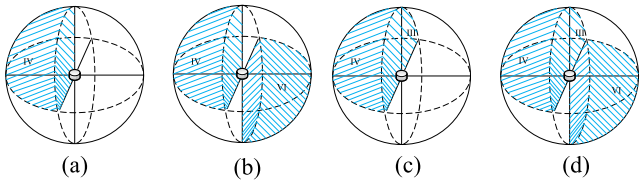

FIGURE 4. Examples for routing void index, where the blue shaded areas are the low-energy warning areas. The routing void index of nodes in (a) and (b) are 1/8 and that of nodes in (c) and (d) are 2/8.

section, the repairing position calculation and the routing void prediction are for the area that contains nodes at the beginning.

D. BASIC IDEA

Our RVPR algorithm enables nodes to predict routing voids nearby, and then the node foreseeing voids asks AUVs to come to repair the voids in time. To achieve the routing void prediction based on the Markov chain model, nodes need to know the communication history of their neighbors and the time of prediction. Thus, the communication history is added in DATA packet. The time of prediction is the time that the AUV spends from its current location to the repair position, which means what the node predict is that the routing void condition when the AUV arrives at the repair position assuming it starts to come now. Therefore, the prediction time can be calculated with the AUV position, the repair position and the AUV's speed. The repair position is solved by PSO algorithm, at which the newly deployed node enables to maximize the void area connectivity and minimize the AUV moving distance. To successfully ask AUVs to repair the voids, nodes and AUVs need reliable and energy-efficient interaction mechanism. When an AUV receives multiple tasks, to ensure that the AUV chooses the most urgent and important one, we device the task selecting rule according to routing voids, node importance and AUV moving distance.

The overall procedure of RVPR algorithm is illustrated in the Fig.5, which mainly contains four parts to achieve the four subtasks described in *PROBLEM STATEMENT*. Firstly, in the repair position calculation phase, nodes exchange two-hop position information during initialization. Meanwhile, AUVs periodically broadcast their position by HELLO packet in a local area. Also, nodes listen to the link information of its neighbors during packet transmission. RVPR algorithm runs if the current link changes. According to the link information and the AUV's position, nodes calculate the repair position. Secondly, in the routing void prediction phase, nodes predict neighbors' energy and the routing void index is calculated. If the predicted value is bigger than 0, the node sends REQUEST packet to the AUV. Thirdly, in the dynamic task selection phase, the AUV selects the most urgent and important task to perform after receiving the REQUEST packet and sends the AGREE packet to the node. The fourth part is information exchange among AUVs and nodes, which runs through the entire RVPR algorithm.

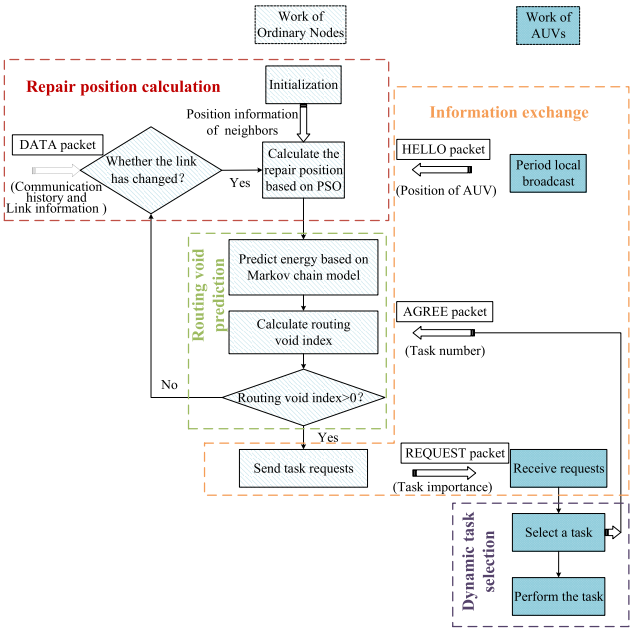

FIGURE 5. Overview of the proposed RVPR algorithm. The propose RVPR mainly consists of four parts: repair position calculation, routing void prediction, dynamic task selection and information exchange. The work of AUVs and the work of ordinary nodes are illustrated by different fill patterns.

IV. THE RVPR ALGORITHM DESIGN

In this section, we discuss the details of RVPR. As mentioned in section III, we can divide the whole algorithm into four parts: repair position calculation, routing void prediction, dynamic task selection and information exchange. Finally, we end this chapter with overhead analysis.

A. REPAIR POSITION CALCULATION

In order to ensure that routing void repairing is timely, ordinary nodes need to calculate the repair position preparing for the possible arrival of the AUV. The target functions are established in two aspects. One is that the position needs to restore as many links as possible once the area becomes the low-energy warning area. The other is to minimize the moving distance of the AUV to reduce the impact on the its daily work. The optimization problem is solved by PSO algorithm.

1) RESTRICTIONS

Assume that the neighbor set of node n_i is $Neighbor_i = \{n_{i1}, n_{i2}, \ldots n_{ij}, \ldots\}$, and the node deployed by the AUV is n_{AUV}. The node n_i queries the link records by region, such as the two-hop links with the neighbors in area I as the relay nodes. There are two kinds of two-hop links, which are the current two-hop link and the other history two-hop links. Next, we establish the equation for each of them.

For the current two-hop link between n_i and n_{ijm}, we record the link as $n_i - n_{ij} - n_{ijm}$ where n_{ij} is assumed to exhaust its energy. In order to restore the connectivity, the position calculation needs to satisfy the signal-noise-ratio threshold

of the receiver. Thus, the following formula is established combining with the acoustic communication model in the section III. B.

$$\begin{aligned} &s.t. \\ &C1. \quad TL_{n_i n_{AUV}} < TL_{th1} \\ &C2. \quad TL_{n_{AUV} n_{ijm}} < TL_{th2} \end{aligned} \tag{6}$$

where $TL_{th1} = SL_1 - NL_1 + DG_1 - Th_{receiver1}$ and $TL_{th2} = SL_2 - NL_2 + DG_2 - Th_{receiver2}$. Thus, the position set S_m is got from (6).

For each of the other two-hop links in area I, we record the link as $n_i - n_{ip} - n_{ipq}$ where n_{ip} is assumed to exhaust its energy. To restore the connectivity of the link, similarly, we have

$$\begin{aligned} &s.t. \\ &C1. \quad TL_{n_i n_{AUV}} < TL_{th1} \\ &C3(x). \quad TL_{n_{AUV} n_{ipq}} < TL_{thx} \end{aligned} \tag{7}$$

where x is the label of the link and $TL_{thx} = SL_x - NL_x + DG_x - Th_{receiverx}$. Thus, the position sets S_x are got from (7).

Considering the current two hop link is more important than the other history links in the network and to restore as many links as possible in the area, the repair position should be able to recover the current link $n_i - n_{ij} - n_{ijm}$ and as many history links $n_i - n_{ip} - n_{ipq}$ as possible. Thus, the constraint S_{repair} is to find a set which is the intersection of S_m and as many S_x as possible. For convenience, we suppose $x = k$, $p = P$ and $q = Q(P \neq j$ or $Q \neq m)$ and therefore $S_{repair} = S_m \cap S_k$. Next, we build objective functions for link $n_i - n_{AUV} - n_{ijm}$ and $n_i - n_{AUV} - n_{iPQ}$ in the next section.

2) OBJECTIVE FUNCTIONS

There are two aspects in the objective functions. First, to ensure the quality of links, we minimize the signal loss among nodes and the newly deployed node. The objective functions are

$$F_1 = TL_{n_i n_{AUV}} \tag{8}$$

$$F_2 = TL_{n_{AUV} n_{ijm}} \tag{9}$$

$$F_3^k = TL_{n_{AUV} n_{iPQ}} \tag{10}$$

In addition, for the AUVs, the closer to the positions deploying nodes, the less impact on the conventional tasks. Thus, we minimize the moving distance as follows:

$$F_4 = \sqrt{(x - x_{AUV})^2 + (y - y_{AUV})^2 + (z - z_{AUV})^2} \tag{11}$$

where $(x_{AUV}, y_{AUV}, z_{AUV})$ is the position of the AUV.

The objective functions of links and AUVs are normalized by linear weighted summation as shown in (12):

$$\begin{aligned} \min \Bigg\{ &\alpha_1 \frac{F_1 - F_1^{\min}}{F_1^{\max} - F_1^{\min}} + \alpha_2 \frac{F_2 - F_2^{\min}}{F_2^{\max} - F_2^{\min}} \\ &+ \alpha_3^k \frac{F_3^k - F_3^{k^{\min}}}{F_3^{k^{\max}} - F_3^{k^{\min}}} + \alpha_4 \frac{F_4 - F_4^{\min}}{F_4^{\max} - F_4^{\min}} \Bigg\} \\ s.t.\ &C1.(x, y, z) \in S_{repair} \end{aligned} \tag{12}$$

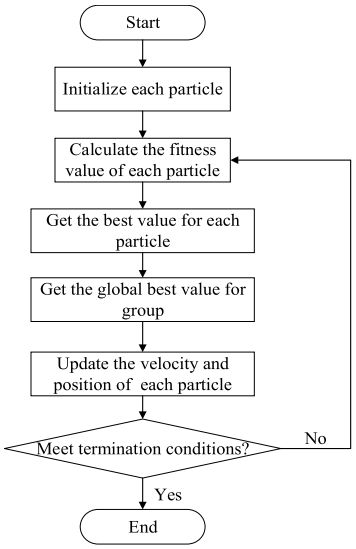

FIGURE 6. Particle Swarm Optimization algorithm.

where $F^{\max}$ and $F^{\min}$ are set according to their physical meanings and the sensor performances. $F_1^{\max}$, $F_2^{\max}$ and $F_3^{k^{\max}}$ represent the maximum attenuation when the signal can still be heard by receiver. Thus, they are set to TL_{th1}, TL_{th2} and TL_{th3} respectively. $F_1^{\min}$, $F_2^{\min}$, $F_3^{k^{\min}}$ are the minimum attenuation between nodes and set to zeros. $F_4^{\max}$ is the longest Euclidean distance along the trajectory of the AUV while $F_4^{\min}$ is 0. $\alpha_1, \alpha_2, \alpha_3^k, \alpha_4$ are the weight coefficients that meet $\alpha_1 + \alpha_2 + \alpha_3^k + \alpha_4 = 1$ $(\alpha_1, \alpha_2, \alpha_3^k, \alpha_4 \geq 0)$.

3) PSO ALGORITHM

Particle Swarm Optimization (PSO) algorithm is a population-based optimization technique inspired by social behavior of bird flocking and roosting. In PSO, individual swarm members establish a social network and can profit from the discoveries and previous experience of the other members of the swarm. PSO is a very efficient global search algorithm and it is computationally light. Thus, we introduce the PSO algorithm to calculate the position to deploy the node. The procedure of the PSO algorithm is shown in Fig.6.

The particles are used to simulate birds. Each particle can be regarded as a search individual in the search space. The particles have two attributes. One is the speed, which represents the speed of movement. The other is the position, which represents the direction of movement. Through iteration, the best values of each particle as well as of the group are calculated. Also, the particles update their speeds and positions. Finally, the global best value that satisfies the termination condition is obtained. Generally, the termination condition is that the maximum number of iterations is reached or the global best value meets the threshold.

The PSO algorithm is a meta-heuristic technique-based algorithm. Almost all meta-heuristic algorithms are simple in terms of complexity, and thus they are easy to implement [30]. Specifically, the complexity of the PSO algorithm is $O(NP{\cdot}D)$

in each iteration [31], where NP is number of the particles and D is the dimension of the objective function. In addition, the nodes underwater have enough storage and computing ability [32]. Thus, the algorithm is feasible considering it is simple in terms of complexity.

B. ROUTING VOID PREDICTION

In RVPR, nodes listen to the channel and record their neighbors' states. They assume the AUV comes to the repair position now and predict the routing voids when the AUV arrives. It is necessary for nodes to predict the routing voids. One reason is that nodes will be no longer able to send information once the routing void is already formed. In addition, since the speed of AUV is low, it will take a certain time to reach the repair position. If the AUV is requested after the routing void has already formed, packets will be lost during the certain time. Thus, we propose a routing void prediction model based on Markov chains.

The Markov process mainly studies the current state of things and the process of future state transitions. It can make good predictions of state transitions and time series. The Markov process is described by (13).

$$P\left\{X_t = s_i | X_0 = s_{j0}, \ldots, X_{t-1} = s_{j(t-1)}\right\} = P\left\{X_t = s_i | X_{t-1} = s_{j(t-1)}\right\} \quad (13)$$

where $\{s_1, \ldots, s_M\}$ represents the state space. The vector X is the state sequence from time 0 to time N. The probability of being in state X_t at time t depends on the previous state X_{t-1}. Since the Markov chain model can accurately predict the state probability, it is advisable to develop a Markov chain on the node state transition model. Moreover, the energy consumption depends on the node history states, which is also the direct cause of routing voids. Thus, the prediction of node states is equal to the prediction of energy consumption, and thereby can accurately predict routing voids.

In UASNs, nodes usually have 3 states, which are listening, receiving and sending. Nodes in different states have different working power. The inherent relationships of the states are shown in Fig.7.

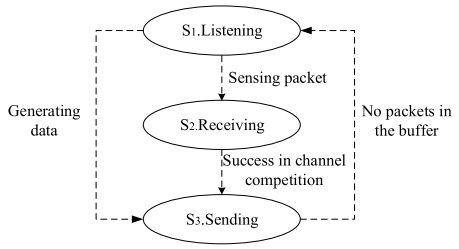

FIGURE 7. Node state transition model.

We divide time into multiple time slots and the nodes are in one state in each time slot. The transition probability from state i to state j is expressed by $P_{ij} = P\{X_t = j | X_{t-1} = i\}$, which can be obtained by statistics on the history states of nodes.

The transition probability from state i to state j can be calculated by (14) after n-time transitions.

$$P_{ij}^{(n)} = \sum_{k=1}^{M} P_{ik}^{r} P_{kj}^{n-r}, \quad (r \in (0, n)) \quad (14)$$

If a node is in state i, $\sum_{t=1}^{L} P_{ij}^{(t)}$ is the number of time slots being in the state j in the next L time slots. Thus, the total energy consumption in the next L slots is

$$E^L = \sum_{j=1}^{M} \sum_{t=1}^{L} P_{ij}^{(t)} \times p(j) \quad (15)$$

where $p(j)$ is energy consumption of nodes in the state j in one time slot.

Then, we can calculate the residual energy of the node when the AUV arrives by (16).

$$E_{res} = E_{ini} - E^L \quad (16)$$

where E_{ini} is the initial energy of nodes. And L can be calculated as (17) by the time that the AUV takes to arrive the repair position.

$$L = [\frac{1}{T} \times \frac{\sqrt{(x_{AUV} - x)^2 + (y_{AUV} - y)^2 + (z_{AUV} - z)^2}}{v_{AUV}}] + 1 \quad (17)$$

where (x, y, z) is the repair position calculated in the repair position calculation phase, v_{AUV} is the speed of AUV and T is the length of the slot.

After that, nodes calculate their own routing void index based on their neighbors' energy that after the L time slots. If it is bigger than 0, the node asks the AUV comes to the repair position.

C. DYNAMIC TASK SELECTION

If an AUV receives multiple tasks, it needs to choose the most urgent and important one. Thus, we design a task selecting rule considering routing void index, node importance and AUV moving distance. The AUV selects the task with the largest value of the task importance defined as:

$$(\alpha_{n_i} + \beta_{n_i}) \cdot \gamma_{n_i} \quad (18)$$

The first part α_{n_i} is the routing void index of the node who generates the task request. Combining with the analysis in the chapter III. C, we know the larger α_{n_i} reflects the routing voids is severer.

The second part β_{n_i} is the importance of the node who sends task requests. Generally, in the acquisition network, if a node is located near the water surface, it will forward packets more frequently comparing with those deployed near the bottom. And thereby it is more important in the network. Thus, we define the node importance as:

$$\beta_{n_i} = 1 - \frac{z_{n_i}}{Z} \quad (19)$$

Type(DATA)	Node ID	Next Forwarder	History States	Data

FIGURE 8. Packet structure of DATA packet.

where z_{n_i} is the depth of the node n_i and Z is the total depth of the monitoring area. We can see that the shallower the node depth, the value of β_{n_i} becomes larger, which reflects the node is more important in the network.

The last part γ_{n_i} is calculated as (20) according to the AUV moving distance. The energy consumption of AUV depends largely on the distance it travels. In addition, to reduce the impact of the AUV performing the original daily task, it should reduce the deviation from the original path. Therefore, AUV moving distance should also be considered.

$$\gamma = \begin{cases} 1 & 0 \le l < l_{safe} \\ 1 - \dfrac{l}{l_{\max}} & l_{safe} \le l < l_{\max} \\ 0 & l \ge l_{\max} \end{cases} \tag{20}$$

where $l_{\max}$ is the maximal distance that a AUV is able to travel, and l_{safe} is the safe traveling distance of the AUV without considering running out of energy, which is always set to the range $\{0.5l_{\max}, 0.9l_{\max}\}$ [33].

D. INFORMATION EXCHANGE

To guarantee the effectiveness of the repair position calculation, routing void prediction and dynamic task selection, we propose a reliable information interaction mechanism with high energy efficiency. In this section, we firstly design the packet structure. Then, we introduce the information exchange among AUVs and nodes.

1) PACKET STRUCTURE

The structure of data packets in the network is depicted in Fig. 8, which is to obtain the information for calculating the repair position and predicting the routing voids. As shown in Fig.8, in addition to the Type, Node ID and Next Forwarder, we add History States in the DATA packet. History States is the record of the node's receiving state. Since all the nodes can sense when the neighbor sends a data packet, the sending states of neighbors can be overheard. Moreover, the listening state can be inferred from the sending and receiving state. Therefore, it is only necessary to record the time when the node is in the receiving state between the two-packet sending interval.

The packet structures of HELLO, REQUEST and AGREE are designed to guarantee information exchange among AUVs and nodes.

The AUVs broadcast the HELLO packet periodically and locally to inform the nodes of their locations. As shown in Fig.9(a), the HELLO packet contains Type, AUV ID, Node ID and AUV Location. It is worth noting that the Node ID is the ID of node who sends the HELLO packet. If the receiving node decides to forward the HELLO packet, the Node ID is saved as the next hop of the future REQUEST packet.

Type(HELLO)	AUV ID	Node ID	AUV Location

(a)

Type(REQUEST)	AUV ID	Node ID	Next Forwarder	Task Number	Task Importance	Repairing Position

(b)

Type(ARGEE)	AUV ID	Task Number	Next Forwarder

(c)

FIGURE 9. Packet structures of HELLO, REQUEST and ARGEE packet.

When the node's routing void index is larger than 0, the node queries the AUV and the corresponding next hop in the record and sends a REQUEST packet. As shown in Fig. 9(b), in addition to Type, AUV ID, Node ID and Next Forwarder, we add Task Number, Task Importance and Repairing Position. Similarly, the Node ID is the ID of node who sends the REQUEST packet. The receiver node records the Node ID as the next hop of the future AGREE packet.

When the AUV receives the REQUEST packet, it will select a task and send the AGREE packet to the node that initiates the request. As shown in Fig.9(c), the AGREE packet contains Type, AUV ID, Task number and Next Forwarder.

2) INFORMATION EXCHANGE AMONG AUVs AND NODES

Firstly, AUVs periodically broadcast their own location information in the network through HELLO packets. The broadcast period is determined by communication range of the ordinary nodes and the speed of the AUVs. Since the speed of the AUV is slow when broadcasting and the communication range is large underwater, the broadcast period is set to tens of seconds to hundreds of seconds generally [10]. After the node receives the HELLO packet, it records the information of the AUV and the node ID that forwards the packet, and then continues to forward the HELLO packet. If the node has received a HELLO packet, when receiving a new one from another AUV, the node will discard the new HELLO packet. Therefore, all nodes store the information of the nearest AUV and the path of the AUV broadcasting message after a round of broadcast. Also, the AUV's information cannot be flooded to the whole network. In other words, the AUV only broadcasts in a local area which contains the nodes closest to itself. For example, as shown in Fig.10, when receiving the information of AUV_2 from n_5, n_4 discards the HELLO packet because it has received the AUV_1 's information from n_3 before. As a result, $n_1 \sim n_4$ receive the information of AUV_1 and $n_5 \sim n_8$ get the information of AUV_2. Thus, the information of AUVs are only flooded locally, which reduces energy consumption as well as ensuring information transmission. In addition, local flooding enables the node to get the information of the nearest AUV, which reduces the AUV moving distance when repairing the voids. If the node does not receive the message from the previously recorded AUV after the time period, then the information of AUV is erased and a new HELLO packet is received to reallocate the AUV's responsible area.

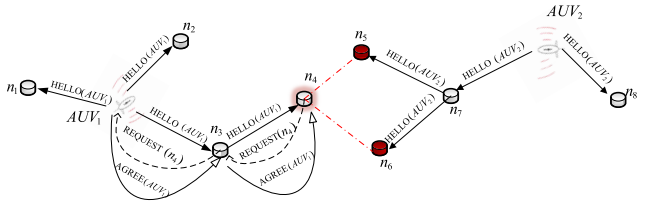

FIGURE 10. Information exchange among AUVs and nodes. We indicate the AUV or node numbers generating the packet in brackets.

Secondly, the node sends a REQUEST packet with Task Importance to the AUV in the record when its predicted routing void index is larger than 0. The REQUEST packet is forwarded following the routing that passes the HELLO packet before. As shown in the Fig. 10, when n_4 predicts that the routing void index is larger than 0, it sends a REQUEST packet to AUV_1 through n_3 in the record.

Lastly, when the AUV receives REQUEST packets, it selects a task to perform according to the task importance and returns the AGREE packet along the former path. As shown in the Fig. 10, AUV_1 sends the AGREE packet to n_4 through n_3 in the record. Meanwhile, the AUV stops broadcasting and goes to the destination with the maximum speed deploying the node to repair the voids.

If the node sending the REQUEST packet receives the AGREE packet within timeout, the node recalculates its own routing void index. If it is still larger than the 0, the node will issue a new REQUEST packet when receiving the HELLO packet of a new AUV. If the AGREE packet is not received, the REQUEST packet is resent when receiving the information of a new AUV.

E. OVERHEAD ANALYSIS

The overhead of the RVPR algorithm mainly comes from the acoustic communications. For the periodic broadcast of AUV, rather than broadcasting to all nodes in the network, AUVs only forwards HELLO packet locally. As a result, the number of flooded HELLO packet is independent of the number of AUVs. In fact, the number of HELLO packet sent is asymptotically $O(n)$ where n is the number of nodes. Also, the broadcast frequency is rather low compared with the packet generation rate. Therefore, the traffic generated by periodic local broadcast is little and acceptable and thereby the collisions are few and the energy consumption is low. In addition, the information exchange between the AUV and the node before performing the task also consumes energy. However, the REQUEST packet and AGREE packet are forwarded along a path with a few hops, which consumes less energy comparing with the daily packet forwarding. Simulation results in the section V show that RVPR has high energy efficiency, which also proves that there is little traffic, few collisions and low energy consumption generated by RVPR.

V. SIMULATION

In this section, we evaluate the performance of the RVPR algorithm. The simulation is carried out from two aspects.

TABLE 1. Simulation parameters.

Name	Value
Initial energy	1000J
Transmission power	10W
Receiving power	3W
Idle power	30mW
Data packet size	50Bytes
Transmission rate	1kbps
Communication range	1000m
Packet generation rate	0.1packet/s
Sound speed	1500m/s
Maximum speed of AUVs	5 knots
Simulation time	5000s

Firstly, we perform the prediction accuracy and the task selection to evaluate the proposed RVPR algorithm. Then, we employ the RVPR algorithm with HHVBF, EAVARP and QELAR to compare the packet delivery ratio (PDR), link connection, end-to-end delay and energy efficiency.

A. SIMULATION SETTING

In our simulations, MATLAB is used as the simulation tool and the acoustic communication model in the section III. *B* is implemented. Varying number of nodes ranging from 50 to 300 and 4 AUVs are evenly deployed in a 5000 m $\times$ 5000 m $\times$ 2500 m three-dimensional space. The network has good connectivity initially. The sensor nodes are identical in every feature, such as initial energy, energy consumption, communication range and so on. We select a source node at the bottom of the network and a surface sink for analysis. The data packet generation follows the independent Poisson distribution process and the rate is 0.1packets/s. The simulation parameters are listed in Table 1.

B. PERFORMANCE EVALUATION

Fig.11 shows the real value of the routing void index of a sample node and the difference between the real value and the predicted one, which prove the accuracy of the routing void prediction mechanism. The sample node is randomly selected from 200 nodes in the network. As shown in the Fig.11, the real value and the predicted value are very similar in most time. In the worst case, the difference between the two values is 1/8. Moreover, we can observe in Fig.11 that the routing void index continues to increase during 1800s to 2500s, which indicates the void will expand once it is formed. Thus, it is very necessary to propose the void repair algorithm to stop the void from expanding.

Fig.12 and Fig.13 depict the effectiveness of the task selecting rules and the PSO-algorithm-based calculation of the void repair position. In Fig.12, we can see that there are 5 tasks $t_1 \sim t_5$ and 4 AUVs$AUV_1 \sim AUV_4$ in the network. AUV_1, AUV_3 and AUV_4 go to the repair positions where are the nearest to them. One reason is that nodes record the nearest AUV when the AUVs locally broadcast their position. Other reason is that the AUVs tend to choose the nearer task to reduce the impact on the daily work. Notice that, AUV_2 selects t_2 to repair instead of t_3. The reason is that

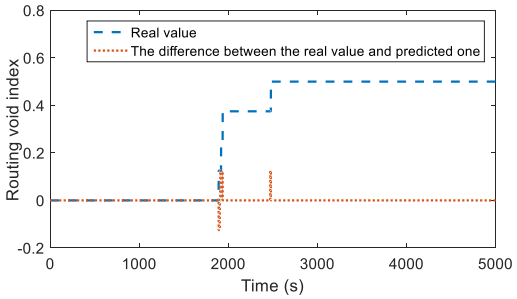

FIGURE 11. Prediction accuracy of a single node.

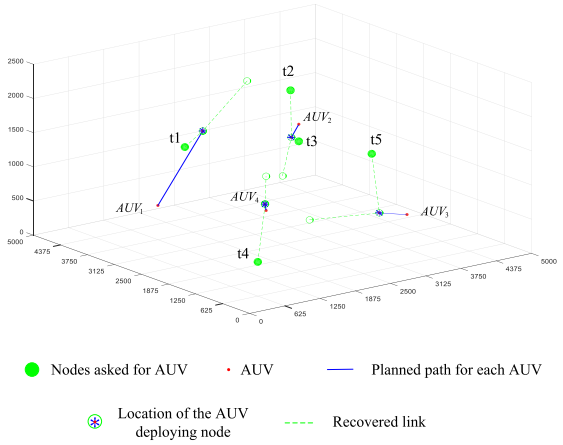

FIGURE 12. Task selection of RVPR.

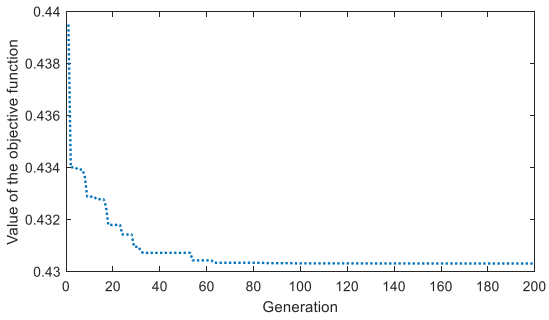

FIGURE 13. Convergence of the PSO algorithm.

our RVPR algorithm considers the node importance when selecting tasks. t_2 is sent by the node located in a shallower position which is also more important. Thus, the AUV_2 goes to perform t_2 although t_2 and t_3 are similar in the routing void index and the AUV moving distance. Fig.13 shows the convergence of the PSO algorithm for task t_1 in the Fig.12. The number of particles is set to 40 and the maximum number of generations is 200 in this paper. We can see that the value of the objective function drops rapidly first and then decreases slowly as the increase of iterations. After about 60 generations, the value changes little which indicates the PSO algorithm converges and the void repairing position is calculated.

Next, we employ the RVPR algorithm with 3 different kinds of routing protocols to evaluate the algorithm

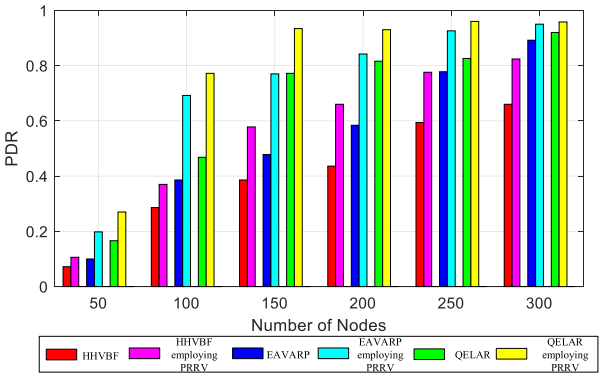

FIGURE 14. Packet delivery ratio according to the number of nodes.

performance. Fig.14 shows the PDR of the routing protocols with and without RVPR according to the number of nodes. We can observe from Fig.14 that the PDR is significantly increased after employing the RVPR algorithm. When the node number is 100, the PDR of HHVBF, EAVAPR and QELAR employing RVPR are increased by 29.4%,79% and 65% respectively. This is because the RVPR algorithm can predict the occurrence of the routing void and ask the AUV to repair it in time. Therefore, RVPR can greatly reduce the packet loss due to routing voids. Moreover, it is observed that the smaller the node number, the RVPR improves the PDR of the routing protocols more significantly, which indicates RVPR is very suitable for sparse-deployed underwater networks. In addition, the PDR continues to grow as the number of nodes increases. This is because there are more nodes can participate in routing, which slows down the formation of routing voids. When the number of nodes is the same, the PDR of QELAR is the highest while that of HHVBF is the lowest. For example, the PDR of QELAR, EAVARP and HHVBF employing RVPR are 77.2%, 69.2% and 37.0% respectively when the node number is 100. This is because QELAR can balance energy consumption and delay the generation of routing voids. However, HHVBF is a greedy- algorithm-based routing protocol and cannot avoid or bypass routing voids. The ability of EAVARP to avoid routing voids is between QELAR and HHVBF. Also, the PDR of the routing protocols are very low when there are only 50 nodes in the network because of the poor network connectivity. For example, the PDR of HHVBF, EAVARP and QELAR are 7.2%, 10.0% and 16.6% respectively. Thus, in order to better test the performance of RVPR, the case of 50 nodes will not be discussed in the following simulations.

Based on the PDR performance of protocols shown in the Fig.14, we simulate and analysis the link connection and end-to-end delay when the node number is 200, because the PDR is not too high or too low under this circumstance, which can well reflect the general law of RVPR. The results are shown in the Fig.15 and Fig.16.

Fig.15 shows the connection of the routing employing different protocols with and without RVPR, where 1 represents connecting and 0 indicates the opposite. It is reasonable to

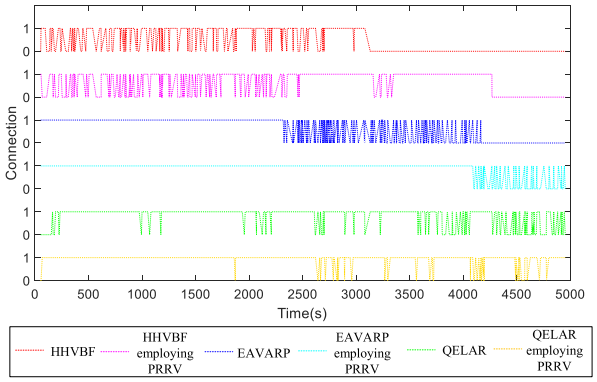

FIGURE 15. Connection according to the time.

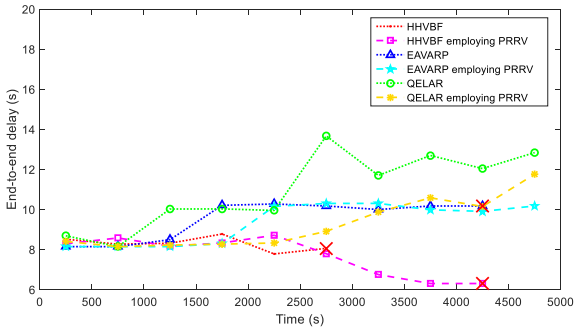

FIGURE 16. End-to-end delay according to the time.

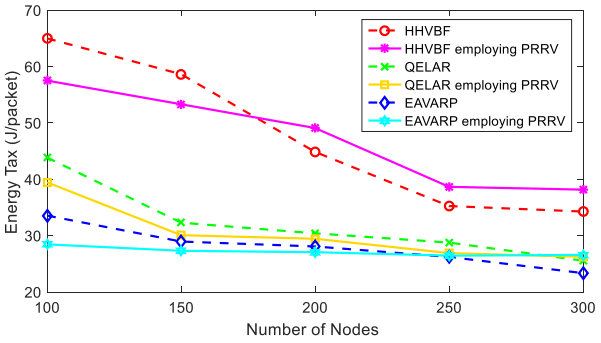

FIGURE 17. Energy tax according to the number of nodes.

believe that short-term link disconnections are due to the characteristics of the protocol and the bit error, and long-term link disconnection and no recovery afterwards is because of routing voids. We can see that for all the different routing protocols, RVPR can repair void area and restore link connectivity in time. For HHVBF and EAVARP, the effectiveness of RVPR is reflected in the longer connection time. For example, the link disconnects after 3131s in HHVBF without RVPR while after 4268s employing RVPR. For QELAR, RVPR reduces the link interruptions because the AUVs deploy new nodes according to the acoustic communication and the convergence of the new routing is quick and easy.

The scenario of Fig.16 is synchronized with Fig.15, which shows the end-to-end delay of different protocols with and without RVPR. In order to facilitate drawing and analysis, we obtain the average end-to-end delay of all the received packets every 500s. It is observed that the end-to-end delay of each protocol employing RVPR is similar to that without RVPR at the beginning. As time goes by, the end-to-end delays perform better than the protocols without RVPR. This is because the protocols try to find the shortest path at first and nodes on this path will run out of energy first, thus, the routing voids are more likely formed on the path, and thereby RVPR is more likely to repair a link with the shortest delay. Moreover, we observe that the end-to-end delay of EAVARP is steady while that of QELAR is on the rise and that of HHVBF is trended down before the link is disconnected. The increase of end-to-end delay indicates the node find a path with more hops. Combining the results in the Fig.15, the link employing QELAR has just a few short disconnects, we can conclude the longer path is to bypass the routing voids. Actually, the end-to-end delay reflects the ability of the protocol to bypass routing voids. QELAR and EAVARP have the ability to bypass the routing voids and HHVBF doesn't. Thus, the link disconnects the earliest when employing HHVBF.

In the next part, we evaluate the energy efficiency of RVPR by energy tax. The energy tax is defined as average energy consumption per packet that is successfully transmitted. Assume E_M is the total energy consumption of sending M packets, and m is the number of packets successfully transmitted to the sink. The energy tax is defined as:

$$E_{tax} = \frac{E_M}{m} \tag{21}$$

From the Fig.17, we can see that the energy tax of each protocol employing RVPR is similar to that without RVPR or even smaller when the node number is small. This is because we consider the energy efficiency when designing the RVPR algorithm. The AUVs only broadcast locally and the information interaction between nodes and AUVs is along the path with the fewest hops. Although RVPR consumes a little extra energy, the PDR is greatly improved due to the effective void repairing. Thus, the energy tax performs well employing RVPR. In addition, we can observe that the performance of EAVARP is better than the other protocols. When the number of nodes is 100, the average energy consumptions are 28.46J/packet when employing RVPR and 33.56 J/packet without RVPR. Also, it remains relatively stable with the number of nodes increases. This is because the PDR increases as the number of nodes increases. The energy tax of HHVBF protocol is the highest because there are too many nodes participating in forwarding packets, which wastes a lot of energy.

VI. CONCLUSION

In this paper, a prediction and repairing of routing voids algorithm over AUV-assisted UASNs is proposed, which provides an effective way to deal with routing voids because of node exhaustion. In RVPR, the void prediction based

on Markov chain model is proposed to ensure the AUV can come to the repair task before the voids has already formed. To maximize the connectivity of the void area and minimize the AUV moving distance, the repair position is calculated based on PSO algorithm. In order to choose the most important and urgent repairing task, we design a task selecting rule according to routing void index, node importance and AUV moving distance. Moreover, RVPR applies an energy-efficient interaction mechanism between nodes and AUVs, which guarantees reliable operation of the algorithm. In the simulation, the RVPR algorithm is employed with several different types of routing protocols (HHVBF, QELAR, EAVARP). The simulation results show that RVPR algorithm enables the routing protocols perform better in terms of the PDR and link connection. Benefit by the proposed RVPR algorithm, when there are 100 nodes deployed in the network, the PDR of HHVBF, EAVAPR and QELAR employing RVPR are increased by 29.4%,79% and 65% respectively.

REFERENCES

[1] *United Nations Website*. Accessed: Oct. 2019. [Online]. Available: https://www.un.org/sustainabledevelopment/oceans

[2] E. Felemban, F. K. Shaikh, U. M. Qureshi, A. A. Sheikh, and S. B. Qaisar, "Underwater sensor network applications: A comprehensive survey," *Int. J. Distrib. Sensor Netw.*, vol. 11, no. 11, Nov. 2015, Art. no. 896832.

[3] M. Jouhari, K. Ibrahimi, H. Tembine, and J. Ben-Othman, "Underwater wireless sensor networks: A survey on enabling technologies, localization protocols, and Internet of underwater things," *IEEE Access*, vol. 7, pp. 96879–96899, 2019.

[4] L. Liu, Y. Liu, and N. Zhang, "A complex network approach to topology control problem in underwater acoustic sensor networks," *IEEE Trans. Parallel Distrib. Syst.*, vol. 25, no. 12, pp. 3046–3055, Dec. 2014.

[5] Z. Jin, M. Ding, Y. Luo, and S. Li, "Integrated time synchronization and multiple access protocol for underwater acoustic sensor networks," *IEEE Access*, vol. 7, pp. 101844–101854, 2019.

[6] Z. Jin, Z. Ji, and Y. Su, "An evidence theory based opportunistic routing protocol for underwater acoustic sensor networks," *IEEE Access*, vol. 6, pp. 71038–71047, 2018.

[7] Y. Noh, U. Lee, P. Wang, B. S. C. Choi, and M. Gerla, "VAPR: Void-aware pressure routing for underwater sensor networks," *IEEE Trans. Mobile Comput.*, vol. 12, no. 5, pp. 895–908, May 2013.

[8] R. W. L. Coutinho, A. Boukerche, L. F. M. Vieira, and A. A. F. Loureiro, "Geographic and opportunistic routing for underwater sensor networks," *IEEE Trans. Comput.*, vol. 65, no. 2, pp. 548–561, Feb. 2016.

[9] K. Latif, N. Javaid, A. Ahmad, Z. A. Khan, N. Alrajeh, and M. I. Khan, "On energy hole and coverage hole avoidance in underwater wireless sensor networks," *IEEE Sensors J.*, vol. 16, no. 11, pp. 4431–4442, Jun. 2016.

[10] S. Yoon, A. K. Azad, H. Oh, and S. Kim, "AURP: An AUV-aided underwater routing protocol for underwater acoustic sensor networks," *Sensors*, vol. 12, no. 2, pp. 1827–1845.

[11] D. Ribas, P. Ridao, A. Turetta, C. Melchiorri, G. Palli, J. J. Fernández, and P. J. Sanz, "I-AUV mechatronics integration for the TRIDENT FP7 project," *IEEE/ASME Trans. Mechatronics*, vol. 20, no. 5, pp. 2583–2592, Oct. 2015.

[12] D. Ribas, N. Palomeras, P. Ridao, M. Carreras, and A. Mallios, "Girona 500 AUV: From survey to intervention," *IEEE/ASME Trans. Mechatronics*, vol. 17, no. 1, pp. 46–53, Feb. 2012.

[13] B. Song, C. Shao, J. Li, and X. Du, "A New Method of Load Separation from Autonomous Underwater Vehicle," *Acta Armamentarii*, vol. 28, no. 2, pp. 146–149, Feb. 2007.

[14] J. Li, P. Wang, X.-M. Wu, B.-W. Song, Y.-H. Cao, and W. Wang, "Analysis of store separation from weapon bay of a Blended-Wing-Body underwater glider," in *Proc. OCEANS-MTS/IEEE Kobe Techno-Oceans (OTO)*, May 2018, pp. 1–5.

[15] P. Xie, J. H. Cui, and L. Lao, "VBF: Vector-based forwarding protocol for underwater sensor networks," in *Proc. Int. Conf. Res. Netw.*, Coimbra, Portugal, May 2006, pp. 1216–1221.

[16] N. Nicolaou, A. See, P. Xie, J.-H. Cui, and D. Maggiorini, "Improving the robustness of location-based routing for underwater sensor networks," in *Proc. OCEANS-Eur.*, Jun. 2007, pp. 1–6.

[17] H. Yan, Z. J. Shi, and J.-H. Cui, "DBR: Depth-based routing for underwater sensor networks," in *Proc. Int. Conf. Res. Netw.*, Singapore, May 2008, pp. 72–86.

[18] T. Hu and Y. Fei, "QELAR: A Machine-Learning-Based adaptive routing protocol for energy-efficient and lifetime-extended underwater sensor networks," *IEEE Trans. Mobile Comput.*, vol. 9, no. 6, pp. 796–809, Jun. 2010.

[19] Z. Wang, G. Han, H. Qin, S. Zhang, and Y. Sui, "An energy-aware and void-avoidable routing protocol for underwater sensor networks," *IEEE Access*, vol. 6, pp. 7792–7801, 2018.

[20] R. W. L. Coutinho, A. Boukerche, L. F. M. Vieira, and A. A. F. Loureiro, "A novel void node recovery paradigm for long-term underwater sensor networks," *Ad Hoc Netw.*, vol. 34, pp. 144–156, Nov. 2015.

[21] R. W. L. Coutinho, L. F. M. Vieira, and A. A. F. Loureiro, "DCR: Depth-Controlled routing protocol for underwater sensor networks," in *Proc. IEEE Symp. Comput. Commun. (ISCC)*, Split, Croatia, Jul. 2013, pp. 453–458.

[22] S. M. Ghoreyshi, A. Shahrabi, and T. Boutaleb, "Void-handling techniques for routing protocols in underwater sensor networks: Survey and challenges," *IEEE Commun. Surveys Tuts.*, vol. 19, no. 2, pp. 800–827, 2nd Quart., 2017.

[23] Y.-S. Chen and Y.-W. Lin, "Mobicast routing protocol for underwater sensor networks," *IEEE Sensors J.*, vol. 13, no. 2, pp. 737–749, Feb. 2013.

[24] G. Qiao, C. Zhao, F. Zhou, and N. Ahmed, "Distributed localization based on signal propagation loss for underwater sensor networks," *IEEE Access*, vol. 7, pp. 112985–112995, 2019.

[25] M. Erol-Kantarci, H. T. Mouftah, and S. Oktug, "A survey of architectures and localization techniques for underwater acoustic sensor networks," *IEEE Commun. Surveys Tuts.*, vol. 13, no. 3, pp. 487–502, 3rd Quart., 2011.

[26] L. Paull, S. Saeedi, M. Seto, and H. Li, "AUV navigation and localization: A review," *IEEE J. Ocean. Eng.*, vol. 39, no. 1, pp. 131–149, Jan. 2014.

[27] H. U. Yildiz, V. C. Gungor, and B. Tavli, "Packet size optimization for lifetime maximization in underwater acoustic sensor networks," *IEEE Trans Ind. Informat.*, vol. 15, no. 2, pp. 719–729, Feb. 2019.

[28] H. Nam, "Data-gathering protocol-based AUV path-planning for long-duration cooperation in underwater acoustic sensor networks," *IEEE Sensors J.*, vol. 18, no. 21, pp. 8902–8912, Nov. 2018.

[29] M. Stojanovic, "On the relationship between capacity and distance in an underwater acoustic communication channel," *ACM SIGMOBILE Mobile Comput. Commun. Rev.*, vol. 11, no. 4, p. 34, Oct. 2007.

[30] X. S. Yang and X. He, "Firefly algorithm: Recent advances and applications," *Int. J. Swarm Intell.*, vol. 1, no. 1, p. 36, 2013.

[31] X. Y. Zhou, Z. J. Wu, H. Wang, K. S. Li, and H. Y. Zhang, "Elite opposition-based particle swarm optimization," *Acta Electron. Sinica*, vol. 41, no. 8, pp. 1647–1652, Sep. 2013.

[32] *AquaSeNt Website*. Accessed: Dec. 2019. [Online]. Available: https://www.aquasent.com/

[33] D. Zhu, H. Huang, and S. X. Yang, "Dynamic task assignment and path planning of multi-AUV system based on an improved self-organizing map and velocity synthesis method in three-dimensional underwater workspace," *IEEE Trans. Cybern.*, vol. 43, no. 2, pp. 504–514, Apr. 2013.

ZHIGANG JIN received the Ph.D. degree in electrical engineering (EE) from Tianjin University, Tianjin, China, in 1999. He was a Visiting Professor with Ottawa University, Ottawa, Canada, in 2002. He is currently a Professor at Tianjin University, Tianjin. His research interests focus on underwater sensor networks, social networks, and deep learning.

QINYI ZHAO received the B.Eng. degree from Tianjin University, China, in 2018, where she is currently pursuing the master's degree. Her main research interest is underwater sensor networks.

YONGMEI LUO received the bachelor's degree from Chongqing University, in 1996. She is currently a Lecturer with the School of Computer Science and Technology, Tianjin University. Her research interest includes networking.